

FLATNESS MEASUREMENTS OF THIN, PLANE-PARALLEL OPTICS FLOATED ON A HEAVY LIQUID

Ulf Griesmann¹, Quandou Wang¹, Johannes A. Soons¹, Eric C. Benck¹,
Jiyoung Chu^{1,2}, and Jaewoong Sohn³

¹National Institute of Standards and Technology,
Gaithersburg, MD 20899, USA

²Samsung Electronics Corp., Suwon-si, Gyeonggi-do, South Korea

³SEMATECH Inc., Albany, NY 12203-3652, USA

INTRODUCTION

The measurement of flatness errors of unconstrained thin parts with low uncertainty is a considerable challenge, because their form is significantly affected by the forces applied through the mechanical fixtures holding them. Forces due to mechanical clamping, chucking in vacuum or electrostatic chucks, and gravity cause surface deformations that must be either eliminated or calibrated.

Absolute tests can sometimes be devised, that permit the separation of instrument errors and mounting-induced errors from the form errors of the part under test. Well known examples are the three-flat tests used for the calibration of interferometer reference flats (see e.g. [1, 2, 3] and the references therein). However, error separation procedures cannot be found for all situations and it is particularly difficult to characterize deformations of a surface due to mounting forces with an absolute test.

We describe a method of separating the intrinsic (or unconstrained) flatness errors of flat precision parts from mounting-induced deformations. Mounting-induced deformations are essentially eliminated when the part is floated on a heavy, high density liquid. The unconstrained flatness error of the part can then be measured directly. The densities of saturated aqueous metatungstate solutions are close to 3 g/cm^3 , which is substantially higher than the densities of many borosilicate crown glasses and important materials with low coefficient of thermal expansion (Table 2), that are used to fabricate precision optics. We illustrate the method with interferometric measurements of the unconstrained flatness errors of silicon and fused silica wafers with a diameter of 300 mm.

An important example of thin, flat optics that must be characterized with very low uncertainty are

photomask substrates and blanks for extreme ultraviolet lithography (EUVL) at a wavelength of 13.5 nm. Photomasks contain the layout of an integrated circuit which is projected, usually demagnified 4:1, onto the wafer surface by an imaging system. EUVL photomask substrates are square with a standard width of 152 mm and a thickness of 6.35 mm. Several low thermal expansion materials (LTEMs) with coefficients of thermal expansion $< 0.03 \times 10^{-6} \text{ K}^{-1}$ are used to make EUVL photomask substrates. Within a quality area of $142 \text{ mm} \times 142 \text{ mm}$, the peak-to-valley flatness error of front- and backsides of an unconstrained EUVL photomask substrate must be as low as 30 nm for the highest quality substrates to achieve the very small pattern placement errors required in EUV lithography. These and other characteristics of EUVL mask substrates are described in a standard published by the Semiconductor Equipment and Materials Industry (SEMI) organization [4]. The method described here was originally developed for measuring the unconstrained flatness error of EUVL photomask blanks and substrates [5].

LITHIUM METATUNGSTATE SOLUTIONS

Lithium metatungstate (LMT), the lithium salt of metatungstic acid with the formula $\text{Li}_6[\text{H}_2\text{W}_{12}\text{O}_{40}] \cdot 3\text{H}_2\text{O}$, is highly soluble in water and other polar solvents [6]. Aqueous solutions of LMT are available commercially for applications requiring separation of materials with different densities, e.g., to separate of fossils from minerals or to separate valuable minerals from sand and clay [7, 8]. Density and viscosity of the tungstate solutions at room temperature depend on the concentration. We chose to use nearly saturated LMT solutions with densities of about 2.95 g/cm^3 . This density is about 30% higher than the density of silica glass and ensures sufficient buoyancy. The properties of the commercially available aqueous LMT solution that are relevant for this application are summarized in Table 1.

TABLE 1. Properties of saturated aqueous lithium metatungstate solutions at room temperature.

Name	Lithium Metatungstate
Abbreviation	LMT
Formula	$\text{Li}_6[\text{H}_2\text{W}_{12}\text{O}_{40}]\cdot 3\text{H}_2\text{O}$
Density ρ [g/cm ³]	2.95
pH	3.2 ± 0.1
Viscosity μ [mPa·s]	36 ± 1
n (632.8 nm, 16.6 °C)	1.5888 ± 0.0002

Metatungstate solutions are stable only when they are acidic [6] (see Table 1). Many glasses are resistant to corrosion when in contact with an acidic solution, but the corrosion resistance of the materials floated on the solution must be considered before a measurement.

The refractive index of a saturated aqueous LMT solution at 2.95 g/cm³ was measured at 632.8 nm, the wavelength of many phase-shifting interferometers used for form measurements, using the minimum deviation method as described by Burnett and Kaplan [9]. A hollow prism with plane parallel windows was filled with the LMT solution and the deviation angles of light passing through the prism at minimum deviation were measured with a goniometer. Deviation angles were measured for light from a helium-neon laser at 632.834 nm and for the red spectral line emitted by a cadmium-argon low pressure discharge lamp at 643.847 nm. The measurements were made at the laboratory room temperature of 16.6 °C. The refractive index of the saturated LMT solution at 632.8 nm and its standard uncertainty, calculated from the standard deviations of the angle measurements, is 1.5888 ± 0.0002 . Since the index n was measured at two closely spaced wavelengths λ , an estimate for the dispersion near 632.8 nm could also be obtained: $dn/d\lambda = (-7.5 \pm 2.6) \times 10^{-5} \text{ nm}^{-1}$. The refractive index of the saturated LMT solution at 632.8 nm is much higher than the index of water (1.332, see [10]) and even slightly higher than the refractive indices of some glasses. For some materials, especially low thermal expansion materials (see Table 2), the index of the LMT solution can be matched to that of glass by diluting the solution with water.

EXPERIMENTAL SETUP

The wafer flatness was measured with the "eXtremely accurate CALibration InterferometerR"

TABLE 2. Densities and refractive indices at 632.8 nm of several glasses and low thermal expansion materials.

Name	ρ [g/cm ³]	n
Fused silica [11]	2.201	1.4570
Schott BK7†	2.51	1.5151
Schott SF5†	4.06	1.6685
Corning ULE 7972†	2.21	1.4840
Schott ZERODUR†	2.55	1.5404
Ohara CLEARCERAM-Z†	2.53	1.5477

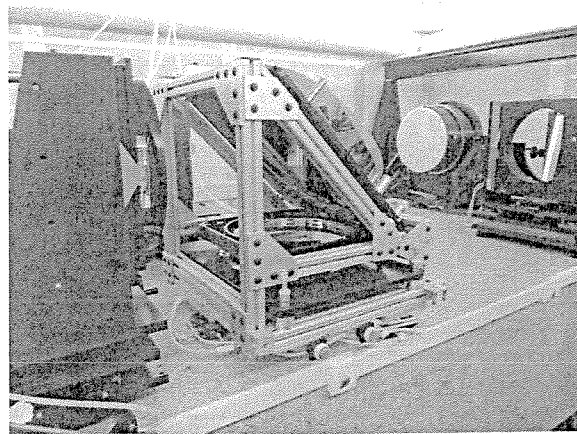


FIGURE 1. Experimental setup using the XCALIBIR interferometer at NIST.

(XCALIBIR) at the National Institute of Standards and Technology (NIST). XCALIBIR is a versatile phase-shifting interferometer operating at a wavelength of 632.8 nm. For the flatness measurements of floating wafers, the interferometer was configured so that the reference flat of the interferometer could be mounted above the photomask in a horizontal orientation. A photograph of the XCALIBIR setup is shown in Fig. 1. The left side of the photograph shows the collimator lens assembly, which creates a collimated test beam of just over 300 mm diameter. The aluminized fold mirror has a diameter of 460 mm and sends the test beam downward to the reference flat, which is visible below the fold mirror in Fig. 1.

A tray machined from an acetal plastic filled with LMT solution was used to float the wafers. Fig. 2 shows a 300 mm diameter silicon wafer floating on a lithium metatungstate solution. In preparation for a flatness measurement, 200 mL of fresh, saturated LMT solution was slowly poured into the tray to avoid the formation of air bubbles and

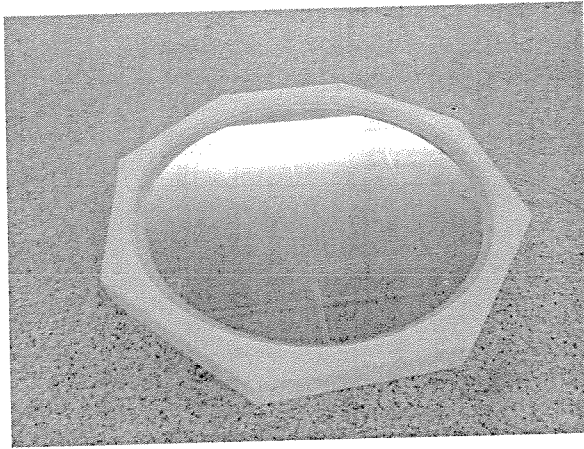


FIGURE 2. A 300 mm diameter silicon wafer floating on a LMT solution.

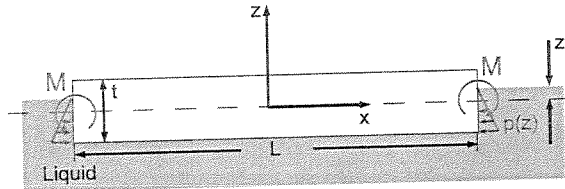


FIGURE 3. Forces and moments acting on a plane-parallel plate floating on a liquid.

the trapping of bubbles at the bottom of the tray. The wafers were then lowered onto the liquid by hand. Three plastic pins were used to prevent lateral movement of the floating parts during measurements. The space between the pins and the wafer is a few tenths of a millimeter to ensure that no force is exerted by the pins on the wafer. Measurements were made immediately after lowering a part onto fresh LMT liquid to avoid problems resulting from water evaporation and crystal formation between the edge of a part and the restraining pins.

While the hydrostatic pressure at the bottom of a floating wafer is constant, a pressure gradient exists at the edges as shown in Fig. 3. The pressure gradient results in a uniformly distributed edge torque M that is balanced by a bending moment of the wafer. The deformation can be calculated analytically for thin plates [12]. The details of the derivation are described in [5].

The equation describing the deformation of a thin plate floating on a liquid by the hydrostatic pres-

sure gradient at the edge is:

$$w(x, y) = \frac{6(1-\nu)g\rho_g}{E} \left(\frac{\rho_g^2}{6\rho_l^2} - \frac{\rho_g}{4\rho_l} \right) (x^2 + y^2), \quad (1)$$

where ρ_g is the density of the glass, ρ_l is the density of the liquid, ν is Poisson's ratio for the glass and E its elastic modulus. The maximum (peak-to-valley) deformation w_m of a square flat with width L is given by:

$$w_m = \frac{3(1-\nu)g\rho_g}{E} \left(\frac{\rho_g}{4\rho_l} - \frac{\rho_g^2}{6\rho_l^2} \right) L^2. \quad (2)$$

Many optical components have a circular shape and it can be shown that the maximum (peak-to-valley) deformation of thin, circular plates with a radius R by hydrostatic pressure gradients at the edge is described by an equation similar to Eq. 1:

$$w_m = \frac{6(1-\nu)g\rho_g}{E} \left(\frac{\rho_g}{4\rho_l} - \frac{\rho_g^2}{6\rho_l^2} \right) R^2. \quad (3)$$

For fused silica $\nu = 0.17$, and $E = 73$ GPa. A fused silica wafer with a 300 mm diameter that is floating on a saturated aqueous LMT solution will have a quadratic deformation of 3.1 nm (peak-to-valley). Similarly, a silicon wafer with a 300 mm diameter ($\rho = 2.33$ g/cm³, $\nu = 0.28$, $E = 185$ GPa) has a deformation of 1.1 nm due to the hydrostatic pressure gradient at the wafer edge.

WAFER FLATNESS MEASUREMENTS

Fig. 4 shows the unconstrained flatness error of an early 300 mm diameter silicon wafer. The wafer shows the characteristic waviness of a wafer that was cut from a silicon boule using a linear wire saw. The wafer in Fig. 5 is made from silica glass and polished with conventional optical polishing methods. The refractive index of the LMT solution was higher than the index of silica glass and the reflection from the back surface of the wafer was attenuated, but not completely eliminated. The attenuation of the unwanted reflection was found to be sufficient for a flatness error measurement of the wafer front surface.

CONCLUSIONS

The flatness error of thin, flexible plane-parallel parts can be measured with low uncertainty when they are floated on a LMT solution, because the part is supported by a uniform pressure that does not distort the shape. The density of saturated lithium metatungstate solutions is sufficiently high

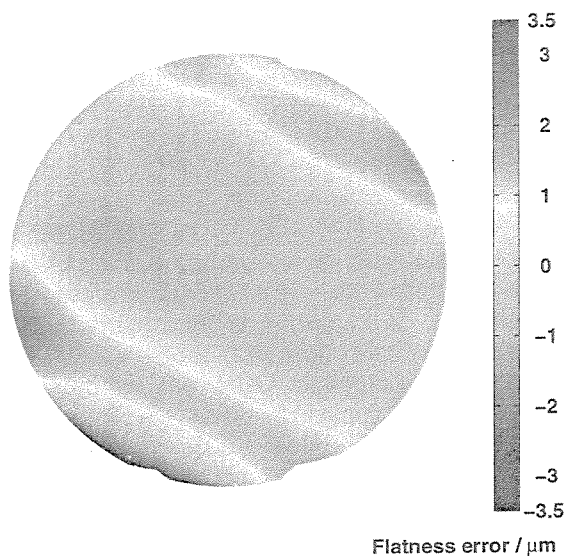


FIGURE 4. Unconstrained flatness error of a 300 mm diameter silicon wafer floating on a LMT solution.

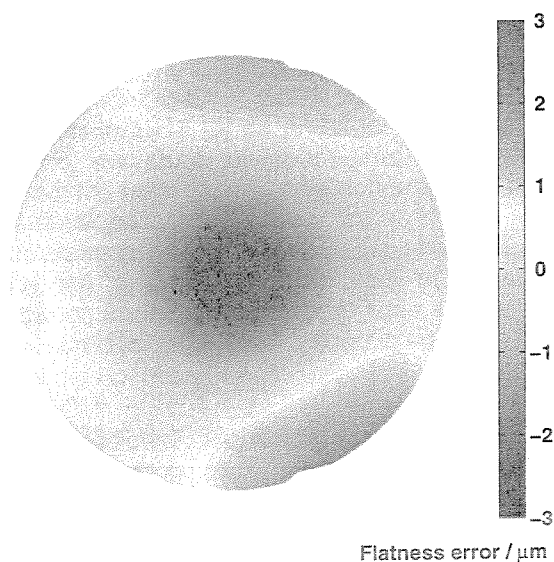


FIGURE 5. Flatness error of a 300 mm diameter silica glass wafer floating on a LMT solution.

to permit lower density glasses to be floated on the heavy liquid. Several important materials with ultra-low thermal expansion can also be floated on LMT solutions. A small quadratic form error results from the hydrostatic pressure gradient at the edge of a floating plate, which leads to a bending moment. The plate bending can be predicted with an analytical model.

†Disclaimer: The full description of the procedures used in this paper requires the identification of certain commercial products and their suppliers. The inclusion of such information should in no way be construed as indicating that such products or suppliers are endorsed by NIST or are recommended by NIST or that they are necessarily the best materials or suppliers for the purposes described.

REFERENCES

- [1] Schwider J. Ein Interferenzverfahren zur Absolutprüfung von Planflächennormalen II. *Optica Acta* 1967: 14, 389–400
- [2] Küchel M. F. A new approach to solve the three flat problem. *Optik* 2001: 112, 381–391
- [3] Griesmann U., Wang Q., and Soons J. A. Three-flat tests including mounting-induced deformations. *Opt. Eng.* 2007: 46, 093601
- [4] SEMI P37-1102, SEMI Standard specification for extreme ultraviolet lithography mask substrates; 2002
- [5] Chu J., Griesmann U., Wang Q., Soons J., and Benck E. C. Deformation-free form error measurement of thin, plane-parallel optics floated on a heavy liquid. *Appl. Opt.* 2010: 49, 1849–1858
- [6] Greenwood N. N. and Earnshaw A. *Chemistry of the elements*, 2nd ed, Butterworth-Heinemann, Oxford; 1997
- [7] Krukowski S. T. Sodium metatungstate; a new heavy-mineral separation medium for the extraction of conodonts from insoluble residues. *J. Paleontology* 1988: 62, 314–316
- [8] Duyvesteyn W. P. C., Liu H., Labaso N. L., and Shrestha P. L. Lithium metatungstate, U.S. Patent 5,178,848; 1993

- [9] Burnett J. H. and Kaplan S. G. Measurement of the refractive index and thermo-optic coefficient of water near 193 nm. *J. Microlithogr., Microfabrication, Microsyst.* 2004: 3, 68–72
- [10] Daimon M. and Masumura A. Measurement of the refractive index of distilled water from the near-infrared region to the ultraviolet. *Appl. Opt.* 2007: 46, 3811–3820
- [11] Malitson I. H. Interspecimen comparison of the refractive index of fused silica. *J. Opt. Soc. Am.* 1965: 55, 1205–1209
- [12] Timoshenko S. P. and Woinowsky-Krieger S. *Theory of plates and shells*, 2nd ed. McGraw Hill, New York, 1959